Surface Reactions of SO_2 With NO_2 on Hydrated Silica and Silica Alumina

by

Stephen Mark Davis

Chemistry

Submitted in Partial Fulfillment of the Requirements of the

University Undergraduate Fellows Program

1976 - 1977

Approved by:

Jack H. Lunsford

Jack H. Lunsford

May 1977

ABSTRACT

Complementary infrared and x-ray photoelectron spectra have been interpreted in a detailed study of surface equilibria involving SO_2, NO_2, N_2O_4, and H_2O adsorbed on amophous silica and silica alumina. Heterogeneous oxidation of SO_2 to sulfuric acid and sulfate ions with NO_2 and water occurs on both surfaces. Reactants adsorb physically initially, and NO_2 forms a reactive nitric acid-like surface complex with adsorbed water. Strongly bound nitrates and nitrites are formed by adsorbing NO_2 onto dehydrated $SiO_2 \cdot Al_2O_3$. The surface reaction with SO_2 at 25° results in an extensive coverage of sulfate ions. Gas phase NO is produced in the reaction, but adsorbed oxo-cations of nitrogen were also detected. These species were identified as NO_2^+ and NO^+ by correlating infrared absorption peaks with N(1s) binding energies. The former ion is stabilized by a shift in acid-base equilibria that accompanies dehydration of the surfaces following the reaction. The latter ion probably exists as ionic $NOHSO_4$, which undergoes surface hydrolysis to H_2SO_4 and NO. Shifts of the bending mode of adsorbed water to higher wavenumbers following the reaction also suggest a strongly acidic surface environment.

ACKNOWLEDGEMENTS

I am immeasurably grateful to Professor Jack H. Lunsford for giving me the opportunity to pursue research at an early stage in my education. Without his financial assistance, understanding, encouragement, and inspiration, this work would not have been possible.

The possibility that NO_2 may oxidize adsorbed SO_2 was suggested to us by Dr. Jack Durham of the EPA. This work was funded by the Environmental Protection Agency under grant number R801136.

Finally, I am indebted to Dr. M. J. Lin for her invaluable assistance with the computations.

TABLE OF CONTENTS

LIST OF FIGURES

LIST OF TABLES

INTRODUCTION

Expanding utilization of coal and lignite as primary fuel sources has prompted pandemic concern over the fate of sulfur dioxide in the atmosphere. The major pollutant is produced during combustion at a rate in excess of seventy billion pounds per year in the United States (1) and oxidized in the atmosphere at a surface interface or photochemically in the gas phase. It was only recently recognized that many solid aerosols adsorb or react with SO_2 in urban regions. Aerosols which contain adsorbed oxides of sulfur have been implicated as causative agents for vegetation damage, reduced visibility, and chronic pulmonary diseases (2,3). For lack of conclusive evidence, the harmful form of sulfur is believed to be the sulfate ion. Of particular importance in this respect are the poorly understood mechanisms through which sulfur dioxide is transformed into surface sulfate ions. Potential oxidizing agents include molecular oxygen, ozone, and nitrogen dioxide.

Several studies have demonstrated that SO_2 is oxidized on common aerosol sources suspended in urban atmospheres. Novakov and co-workers (4,5) reported photoelectron spectra which indicate that both sulfites and sulfates exist on smog particles collected in Pasadena, California. Similar results were reported by Hulett *et al.* in studies with flyash (6), a typical aerosol constituent composed largely of aluminosilicates with iron oxide impurities. The manner in which these surface species are formed, however, remains obscured because complex oxidation processes

---

The citations of the following pages follow the style of *The Journal of Physical Chemistry*.

occur when pollutants interact, and, moreover, aerosols are invariably heterogeneous mixtures of several components.

Results regarding the reactions of SO_2 with model surfaces have recently appeared in an attempt to afford clarification of SO_2 removal from the atmosphere. Since Lunsford's review (7) summarizes these findings through early 1975, only the more revealing consequences will be emphasized here. Infrared studies (8-10) have confirmed that SO_2 chemisorbs on dehydrated magnesium and calcium oxides to form mono- and bidentate surface sulfites. Heating in oxygen at 200° and higher temperatures converts the strongly adsorbed sulfites to sulfate ions. More recently, the surface reaction of H_2S with SO_2 on MgO has been reported to produce water, elemental sulfur, and sulfite ions (11). On acidic polycrystalline aluminosilicate surfaces SO_2 adsorbs physically via strong hydrogen bonding with surface hydroxyl groups (12). Sulfate ions result from the oxidation of SO_2 with humidified air on Fe_2O_3 and MnO_2 (6) or oxygen and water vapor on aluminosilicate-supported transition metal ions (13). Other investigations (10,14-17) have demonstrated that the monovalent oxoanions of sulfur, SO_x^- (x=1-4), may be stabilized on a number of oxide surfaces. These results, not surprisingly, suggest that the observed reactions of SO_2 are highly dependent upon the oxidant and acid-base properties of the support.

No significant results are available regarding the reactivity of adsorbed SO_2 with oxides of nitrogen. This is unfortunate from a practical viewpoint because NO and NO_2 are also common air pollutants. On the other hand, the related gas phase SO_2-NO_2 reactions have attracted continued interest. The results (18,19) generally imply that

photoxidation of SO_2

$$SO_2 + NO_2 \overset{h\upsilon}{\rightleftharpoons} SO_3 + NO \qquad (1)$$

may occur at high concentration levels; however, at atmospheric levels, which are on the order of 10^{-1}-10^{-2} ppm, quenching by molecular oxygen

$$O_2 + NO_2 \overset{h\upsilon}{\rightleftharpoons} O_3 + NO \qquad (2)$$

essentially precludes SO_3 production. In addition, recent evidence (20,21) suggests that photolysis of SO_2-NO_2-air mixtures yields $NOHSO_4$ aerosol which slowly hydrolyzes in air to form sulfuric acid and NO.

The purpose of this study has been to explore the surface reactions of SO_2 and NO_2 on common materials under mild conditions in order to extend the general understanding of the oxidation and removal of SO_2 in the atmosphere. Infrared and x-ray photoelectron spectroscopic studies have been implemented to detect the reactions which occur on hydrated silica and silica alumina. Reviews are available regarding the applications of infrared (22,23) and XPS (24) spectroscopy in surface studies; consequently, theory and experimental details will not be described except where it is essential for interpretation of the data.

EXPERIMENTAL

Amorphous silica gel (Sargent-Welch, 60-200 mesh) and silica alumina (Grace Chem.) were used as supplied. The alumina content of the latter, 9.3±0.2% by weight, was determined gravimetrically by precipitating aluminum oxinate (I) from acidic solutions of

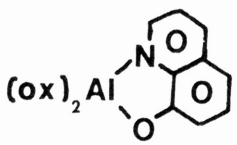

I

Aluminum(III) tris-8-hydroxy quinolate

dissolved catalyst by a method described in more detail elsewhere (25). The BET surface area of the silica alumina, obtained from nitrogen adsorption, was 360±30 m^2/g. Sulfur and nitrogen dioxides were obtained commercially and were purified before use by repeated freeze-pumping at -196° and -23°, respectively.

Samples consisted of transparent wafers (3-8 mg/cm^2) formed in a steel die at a pressure of 2.4×10^3 kg/cm^2. Wafers were mounted on a fused quartz frame and suspended in an infrared or ESCA sample cell. The cells, shown in Figure 1, have been described previously (9). Sample degassing and gas transfers were carried out on a conventional vacuum system operating at 5×10^{-5} Torr, illustrated further in Figure 2. In a typical experiment the cell containing the sample was briefly evacuated until the pressure was less than about 0.1 Torr. Subsequently, either SO_2 or NO_2 was introduced at a desired pressure. After equilibration, usually for about 1 hr, and removal of the excess gas phase by expansion or evacuation, the second gas was admitted at a similar pressure. The surface reaction was allowed to proceed for several

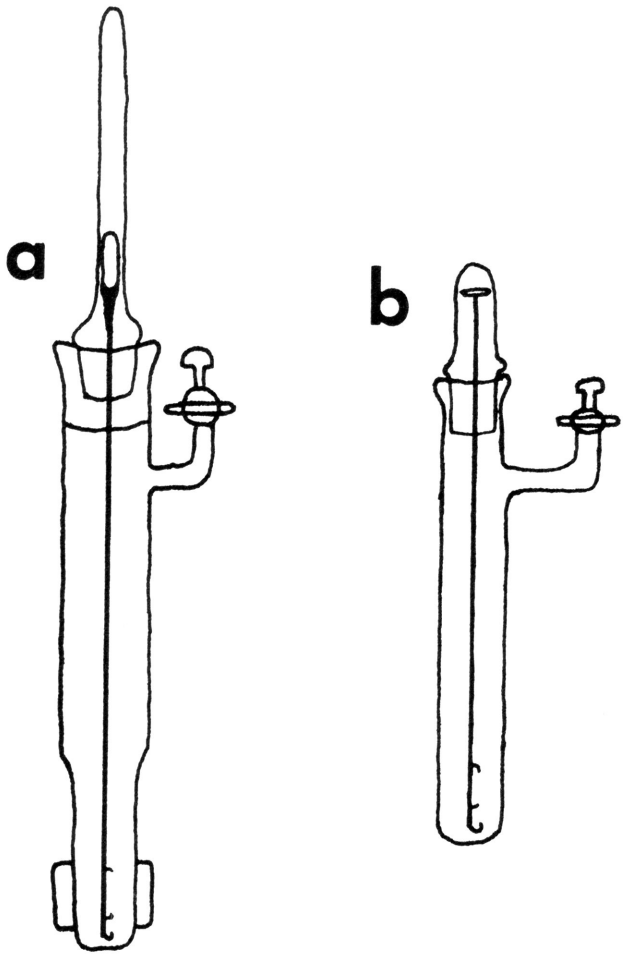

Figure 1. Infrared(a) and ESCA(b) sample cells.

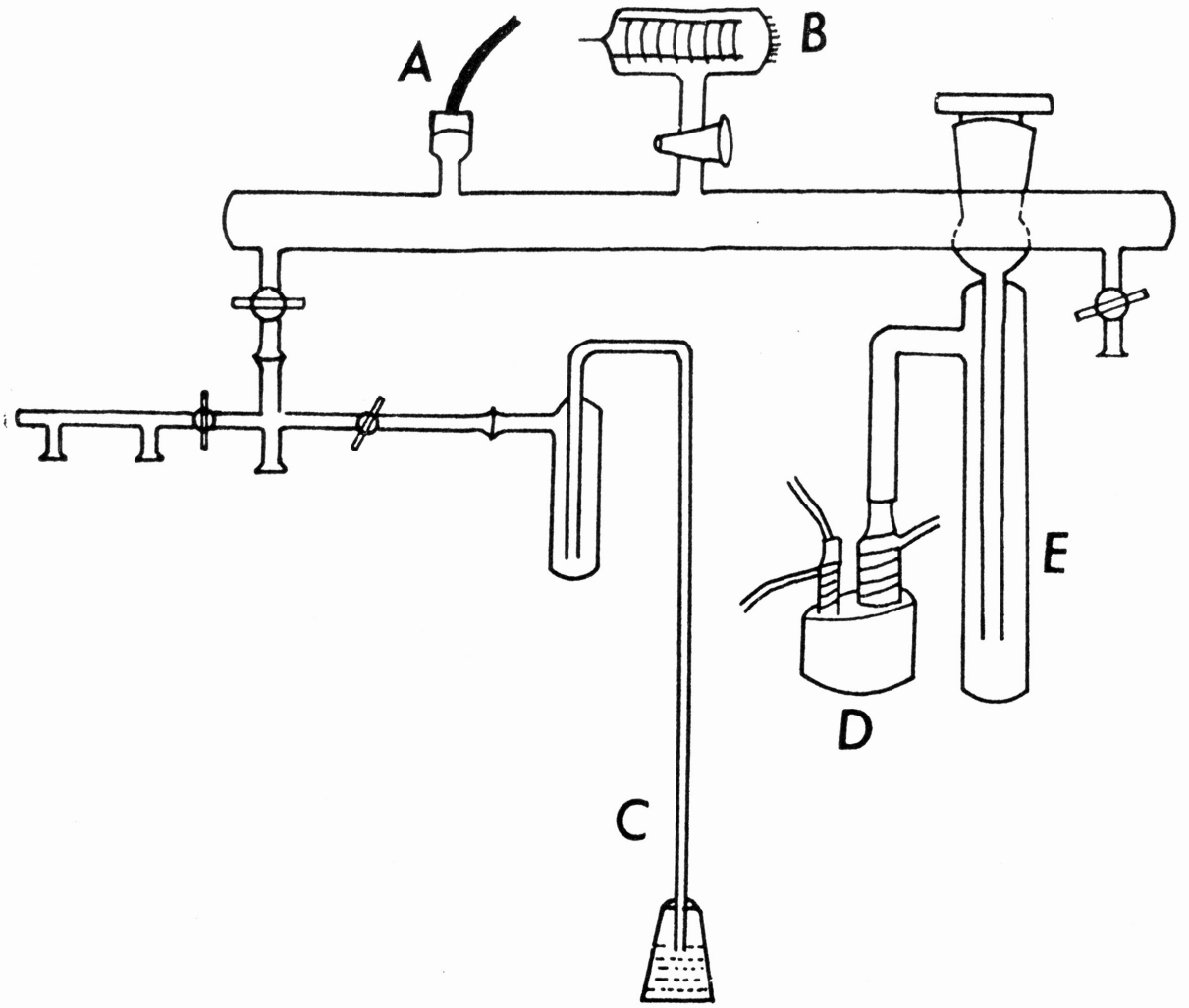

Figure 2. Vacuum system: (A) thermocouple gauge; (B) ionization gauge; (C) mercury manometer; (D) diffusion pump; (E) liquid nitrogen trap.

hours, and the unreacted gas phase was removed by evacuation before transferring the sample into the ESCA spectrometer. Additional experiments were carried out in which samples were dehydrated prior to reaction by heating *in vacuo* to 500° in increments of 100° per hour.

Photoelectron spectra were collected with a Hewlett-Packard 5950A ESCA spectrometer using monochromatic aluminum $K_{\alpha_{1,2}}$ X-radiation (1486.6 eV). Instrumental operation and design along with sample handling techniques for the HP 5950A have been described in detail by Siegbahn and co-workers (26). The pressure in the analysis chamber was maintained below 10^{-8} Torr and all spectra were obtained at 25° or 60°. Excessive positive charging of the surface was neutralized by low energy electrons from a flood gun. Binding energies were referenced relative to the $Au(4f_{7/2})$ level (84.0 eV) of gold which was vacuum sputtered onto the samples. As a second reference, a low intensity C(1s) line at 285.0 eV, resulting from pump oil contamination, was also employed. All measurements were repeated several times with a reproducibility in binding energy of ±0.2 eV. Smoothing and deconvolution of the spectra were accomplished with a five point smoothing program (27) and a Dupont 310 curve resolver utilizing Gaussian lineshapes.

Infrared spectra were recorded with a Beckman IR-9 spectrophotometer operating in the double beam transmittance mode with spectal slit widths of 1-2 cm^{-1} over the range 1200-2500 cm^{-1}. The maximum absolute transmission of each sample was about 60-70%. The spectrophotometer was purged with dry air to remove atmospheric water vapor, but absorption by atmospheric CO_2 obscured the region 2320-2400 cm^{-1}.

EPR spectra, referenced relative to 2,2-diphenyl-1-picrylhydrazyl (g=2.0036), were recorded at -196° using a Varian E6S spectrometer operating at X-band frequencies.

RESULTS

ESCA Studies of Adsorbed Species

Prior to a reaction ESCA spectra for the Al(2p), Si(2p), Al(2s), and Si(2s) lines of silica and silica alumina were characterized by binding energies of 74.3 (Fwhm=1.9 eV), 102.6 (1.9), 119.5 (2.1), and 153.8 (2.2) eV, respectively. Silica exhibited a line of very low intensity in the N(1s) region, whereas SiO_2-Al_2O_3 displayed a broad, moderately strong background line at 401.9 (1.9) eV. No S(2p) photoelectrons were detected from either surface before or after exposure to SO_2, SO_2 and O_2, or SO_2 and air.

As depicted in Figure 3, adsorbed species with N(1s) binding energies of 407.3 and 400.5 eV were formed when 20 Torr NO_2 was admitted to samples for the indicated times. Adsorbate binding energies are given in Table I. The decreasing intensity of these lines with collection time, relative to the background peak at 401.8 eV, indicates that these species were desorbed within the analysis chamber of the spectrometer (pressure$<10^{-8}$ Torr). Desorption of the species responsible for the 400.5 eV line was essentially complete within about 12 hr at 27°, and the peak was not clearly resolved unless the samples were exposed to at least 10-12 Torr NO_2 for a minimum of ca. 30 min.

Markedly different behavior was observed when SO_2 and NO_2 were allowed to react at 25° on the hydrated surfaces. Curve a of Figure 4 was recorded after admitting 25 Torr SO_2 to a silica sample for 4 hr, expanding the excess gas phase to about 2 Torr, and introducing 25 Torr NO_2 for 4 hr. An intense S(2p) line demonstrates that a strongly

Figure 3. N(1s) ESCA spectra for adsorbed NO_2: (a) 20 Torr, exposed to SiO_2 4 hours; (b) 20 Torr, exposed to $SiO_2 \cdot Al_2O_3$ 2 hours; (c) pure NH_4NO_3.

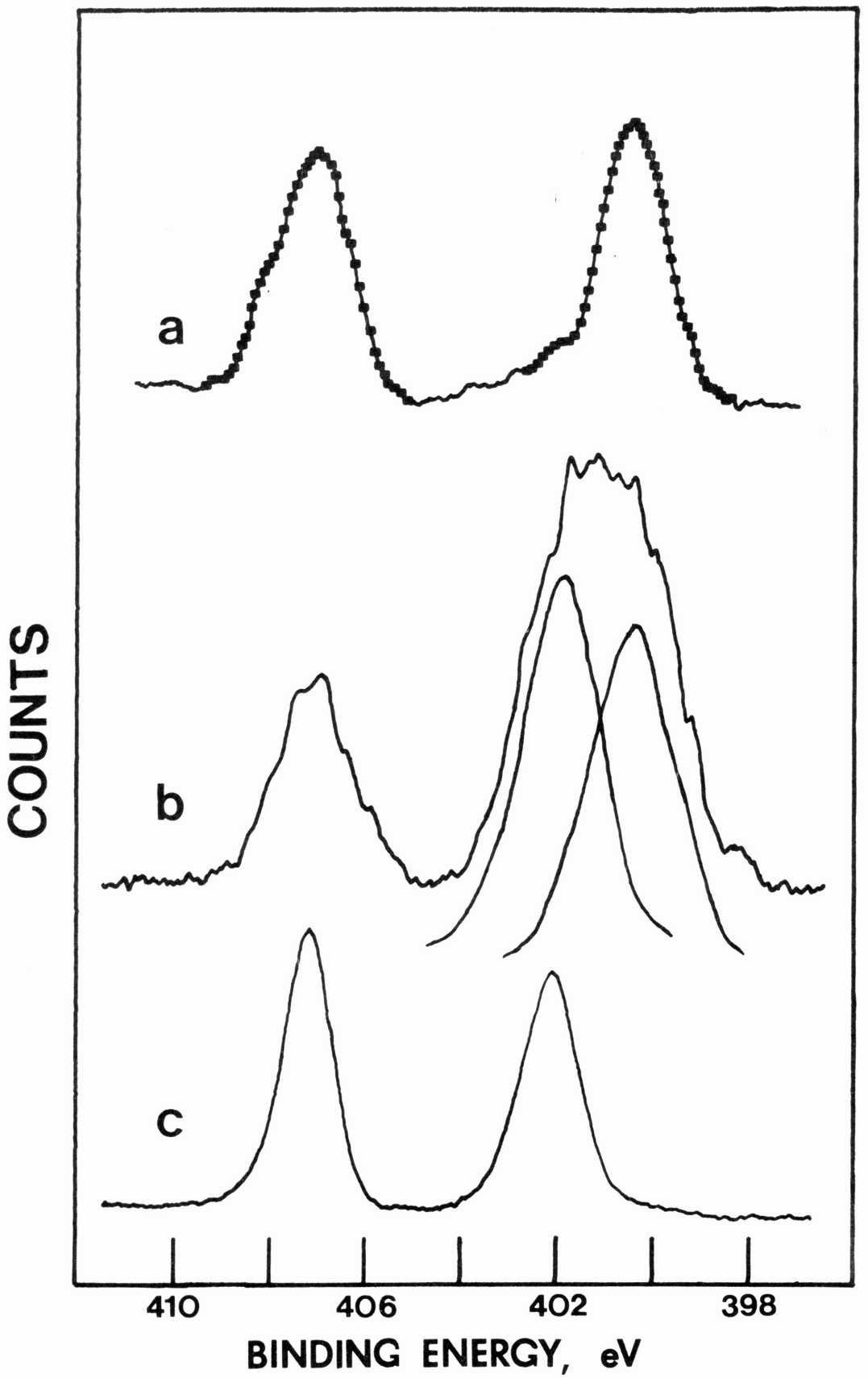
a
b
c
COUNTS
410
406
402
398
BINDING ENERGY, eV

Figure 4. S(2p) and N(1s) ESCA spectra produced by reacting SO_2 with NO_2: (a) SiO_2; (b) $SiO_2 \cdot Al_2O_3$; (c) pure $(NH_4)_2SO_4$.

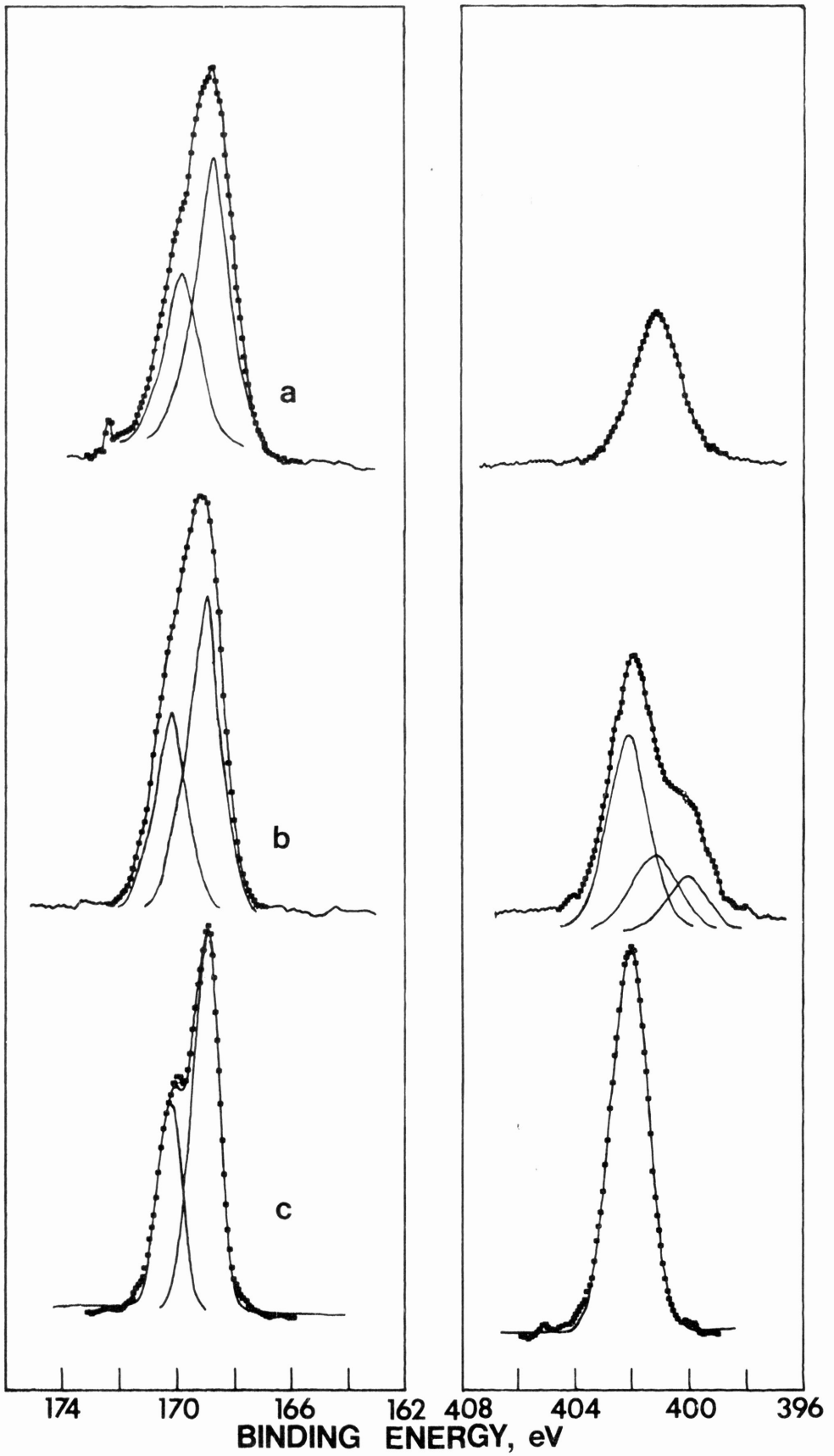
a
b
c
174
170
166
162
408
404
400
396
BINDING ENERGY, eV

Table I. Binding Energies (eV)[a] of Adsorbed Species

Adsorbate	Line	SiO_2	$SiO_2 \cdot Al_2O_3$	Description
background	N(1s)	-	401.9(1.9)	NH_4^+
NO_2	N(1s)	407.2(1.8)[b]	407.3(1.8)	NO_3^-
		400.6(1.9)	400.5(1.9)	phys. ads. N_2O_4
$SO_2 + NO_2$	$S(2p_{3/2})$	168.9(1.4)	168.8(1.4)	
	$S(2p_{1/2})$	169.9(1.4)	169.9(1.4)	$SO_4^=$
	S(2s)	233.1(1.9)	233.0(1.9)	
	N(1s)	401.2(1.8)	401.3(1.8)	NO_2^+
		-	400.5(1.7)	NO^+ ?

a) ±0.2 eV
b) (Fwhm)

bound sulfur oxoanion was formed in the surface reaction. Likewise, curve b illustrates spectra collected from a hydrated $SiO_2 \cdot Al_2O_3$ sample after admitting 8 Torr SO_2 for 20 min, expanding the excess to less than 1 Torr, and, subsequently, adding 8 Torr NO_2 for 4 additional hr. Both samples were in the spectrometer about 12 hr at 60° before collecting the N(1s) spectrum, and desorption of the residual species was not detected. For comparative purposes, curve c depicts the S(2p) and N(1s) ESCA spectrum for $(NH_4)_2SO_4$. The $2p_{3/2}$ and $2p_{1/2}$ binding energies in each spectrum are very close to 168.9 and 169.9 eV, respectively. Significantly, no N(1s) photoelectrons with binding energies of 407 eV were detected from samples following the surface reaction, even when the nitrogen spectrum was recorded immediately after loading the sample into the spectrometer.

Similar binding energies, but with generally less intense lines, were observed when lower pressures or shorter reaction times were used. No S(2p) line was discernible from samples degassed longer than about 30 sec prior to admission of NO_2, and samples maintained in darkness throughout the experiment gave the same spectrum as those in ordinary laboratory light. Consideration of the relative intensities of the N(1s) and S(2p) peaks from a large number of samples following the surface reaction verifies that adsorbed sulfur is ordinarily present in higher concentrations than adsorbed nitrogen. The only exception to this rule occurred with samples which were pretreated with a low pressure of SO_2 and subsequently with a much higher pressure of NO_2. From the ESCA spectra of pure compounds the relative N(1s) to S(2p) photoelectric cross section for our spectrometer was determined to be

0.49±0.10. Using this figure and experimental intensity ratios of N(1s) and S(2p) lines the sulfur:nitrogen surface stoichiometry was found to vary approximately between 5-10:1, 3-5:1, and 0.5-3:1, for samples reacted first with NO_2, with NO_2 and SO_2 mixtures, and first with SO_2, respectively.

Surface coverages of sulfur and nitrogen were highest on samples which were reacted with mixed gases. Furthermore, sulfur and nitrogen surface coverages were consistently higher on silica alumina. Figure 5a displays the Si(2s) and Al(2s) region of a fresh $SiO_2 \cdot Al_2O_3$ sample, whereas curve b shows the same region after a sample was reacted 3 hr with 1 atm of air enriched to 0.7% (5 Torr) in SO_2 and NO_2. The second spectrum demonstrates the relatively rapid SO_2 oxidation at modest pressures to an extensive surface coverage ($\theta \sim 0.9$) of sulfate ions. Interestingly, the Si(2s and 2p) lines were dramatically attenuated to about 8% of their initial intensities, but the Al(2s) intensity was reduced by only about 10%. This behavior was quite general on all $SiO_2 \cdot Al_2O_3$ samples examined with high coverages of sulfate ions. Assuming a cross-sectional area of $24 \mathring{A}^2$, the sulfate surface coverage corresponds to an uptake of about 2 mmole of SO_2 per gram of catalyst.

Infrared Studies of Adsorbed Species

Figure 6 shows the spectra observed for a hydrated silica sample during various stages of adsorption and reaction of SO_2 with NO_2-N_2O_4. The background peak at 1635 cm^{-1}, curve a, is due to absorption by physisorbed water. Except for windows of relatively low transmission between 500-700 and 900-1000 cm^{-1}, both SiO_2 and $SiO_2 \cdot Al_2O_3$ are infrared opaque

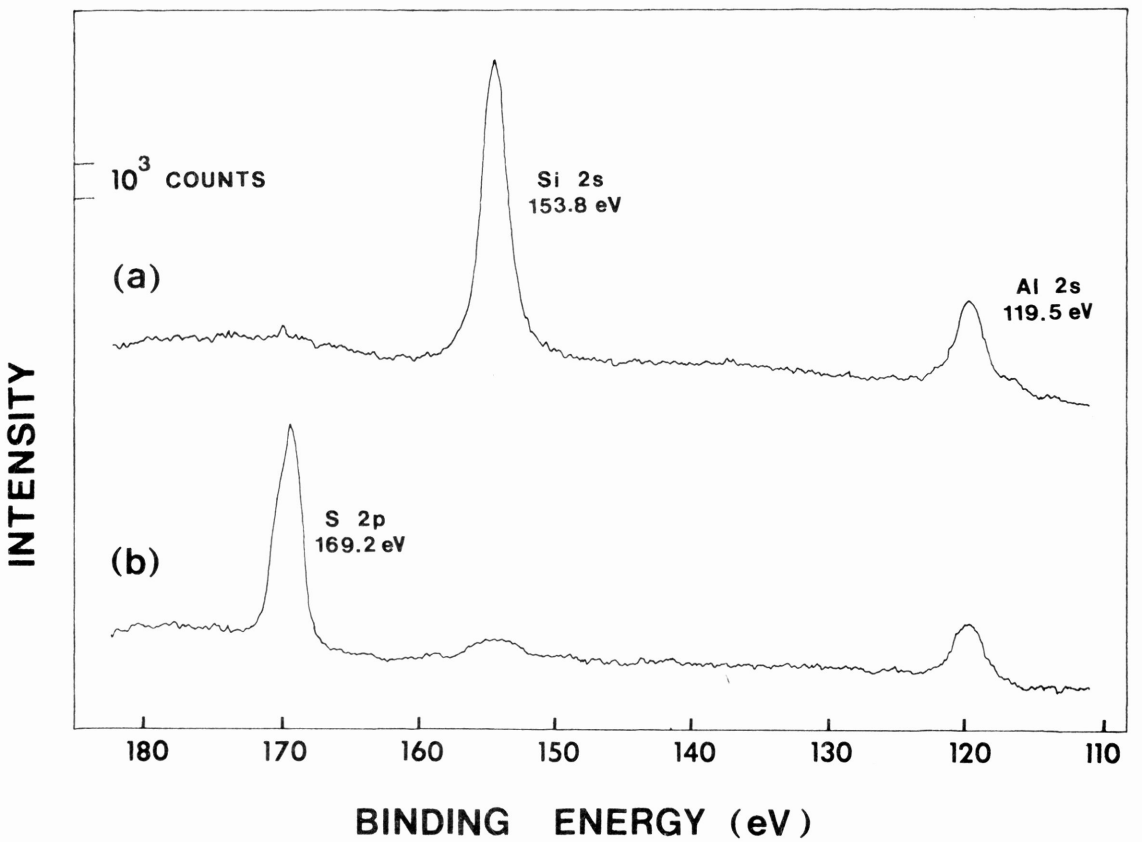

Figure 5. ESCA spectra produced by reacting SO_2 with NO_2 on $SiO_2 \cdot Al_2O_3$: (a) background; (b) after 3 hr reaction with one atm of air enriched to 0.7% with SO_2 and NO_2.

below about 1260 cm^{-1}. Curve b shows a low intensity, physically adsorbed SO_2 band at 1337 cm^{-1}, in equilibrium with gas phase SO_2 which appeared following admission of 5 Torr SO_2 for 20 min and expansion of the excess SO_2 to about 2 Torr. Upon further exposure to 7 Torr (solid curves) or 18 Torr NO_2-N_2O_4 (dashed curves) in an independent experiment, curve c, bands were produced at 1315(sh), 1680, 2280, and 1735 cm^{-1}. The latter band grew slowly in intensity. These peaks, as well as those at 1400 and 2460 cm^{-1} which appeared after degassing 3 hr at 25°, curve d, were all enhanced by higher NO_2-N_2O_4 pressures. The 2460 cm^{-1} band broadened and the 1400 cm^{-1} peak vanished after readsorbing water vapor, curve e, but both could be restored by further outgassing at 25°.

A broad shoulder slowly appeared at 1425 cm^{-1} in addition to bands at 1315(sh), 1680, and 1735 cm^{-1} when silica samples were exposed to NO_2-N_2O_4. The peak at 1420 cm^{-1} sharpened while the other bands were removed after degassing at 100° for 1 hr. The bands at 2280 and 1400 cm^{-1} were never observed unless SO_2 and NO_2 were allowed to react, and the latter appeared only after the sample was degassed at 25° for 1 hr or more.

Figure 7 illustrates more clearly the reactivity of physisorbed NO_2 and N_2O_4 with SO_2 on hydrated silica. Curve a was obtained after admitting 8 Torr NO_2-N_2O_4 to the sample for 45 min. and briefly (1-2 sec.) evacuating the excess gas phase. Subsequent exposure to 8 Torr SO_2, curve b, resulted in disappearance of the 1315 and 1680 cm^{-1} bands and, slowly, a reduction in intensity of the 1735 and 1635 cm^{-1} peaks. Degassing at 25° overnight, curve d, produced a band at

Figure 6. Infrared spectra of SO_2 and NO_2 on hydrated SiO_2: (a) background; (b) 5 Torr SO_2 added 20 min with excess expanded to about 2 Torr; (c) 7 Torr NO_2-N_2O_4 admitted 30 min (broken curves are for a pressure of 18 Torr); (d) degassed at 25° 3 hr (6 hours); (e) 8 Torr H_2O adsorbed.

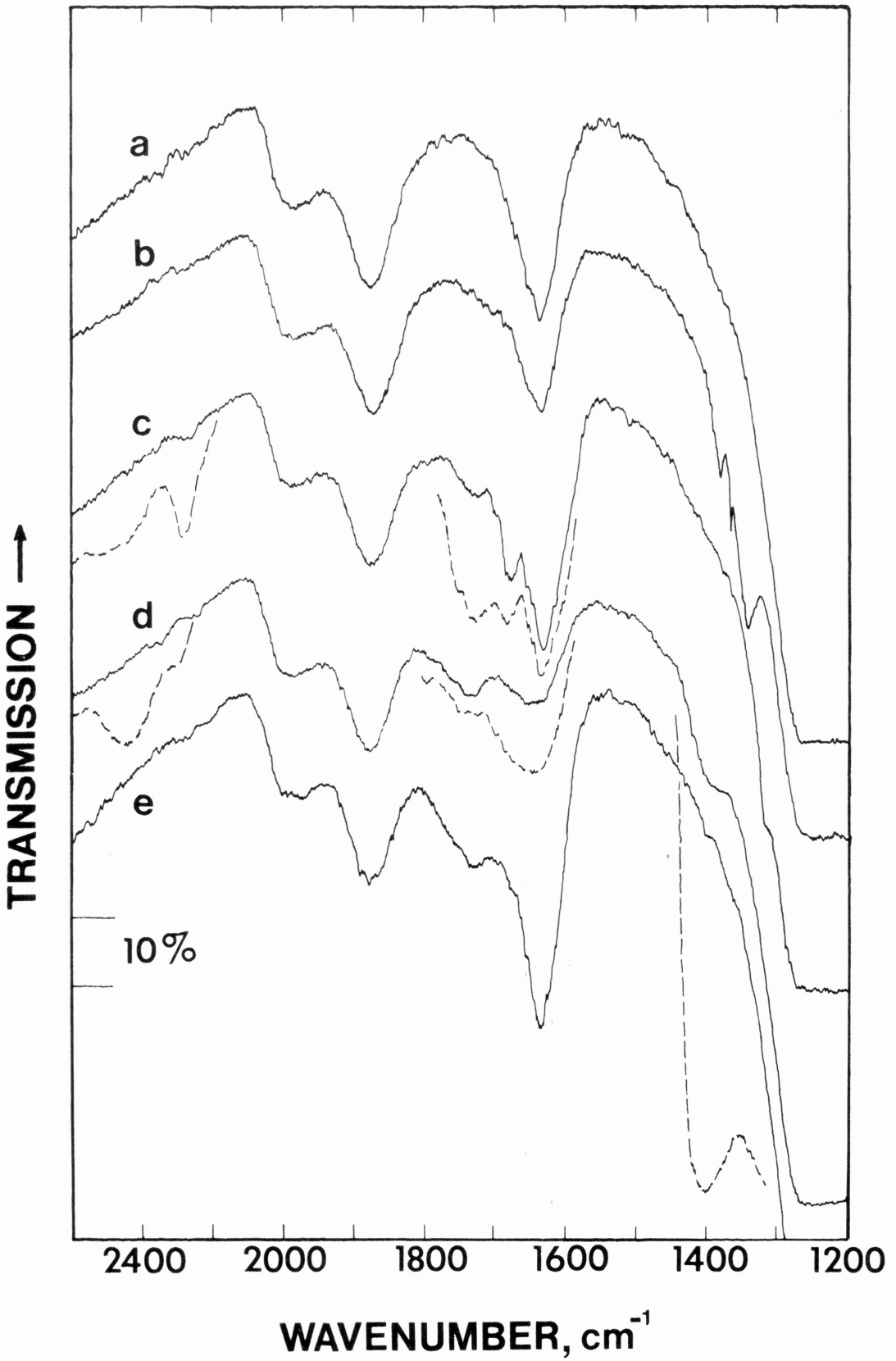
a
b
c
d
e
10%
TRANSMISSION
2400
2000
1800
1600
1400
1200
WAVENUMBER, cm^{-1}

Figure 7. Infrared spectra of NO_2 and SO_2 on hydrated SiO_2: (a) 8 Torr NO_2-N_2O_4 admitted 45 minutes with excess removed; (b) 8 Torr SO_2 admitted; (c) 4 hr later; (d) degassed overnight at 25°.

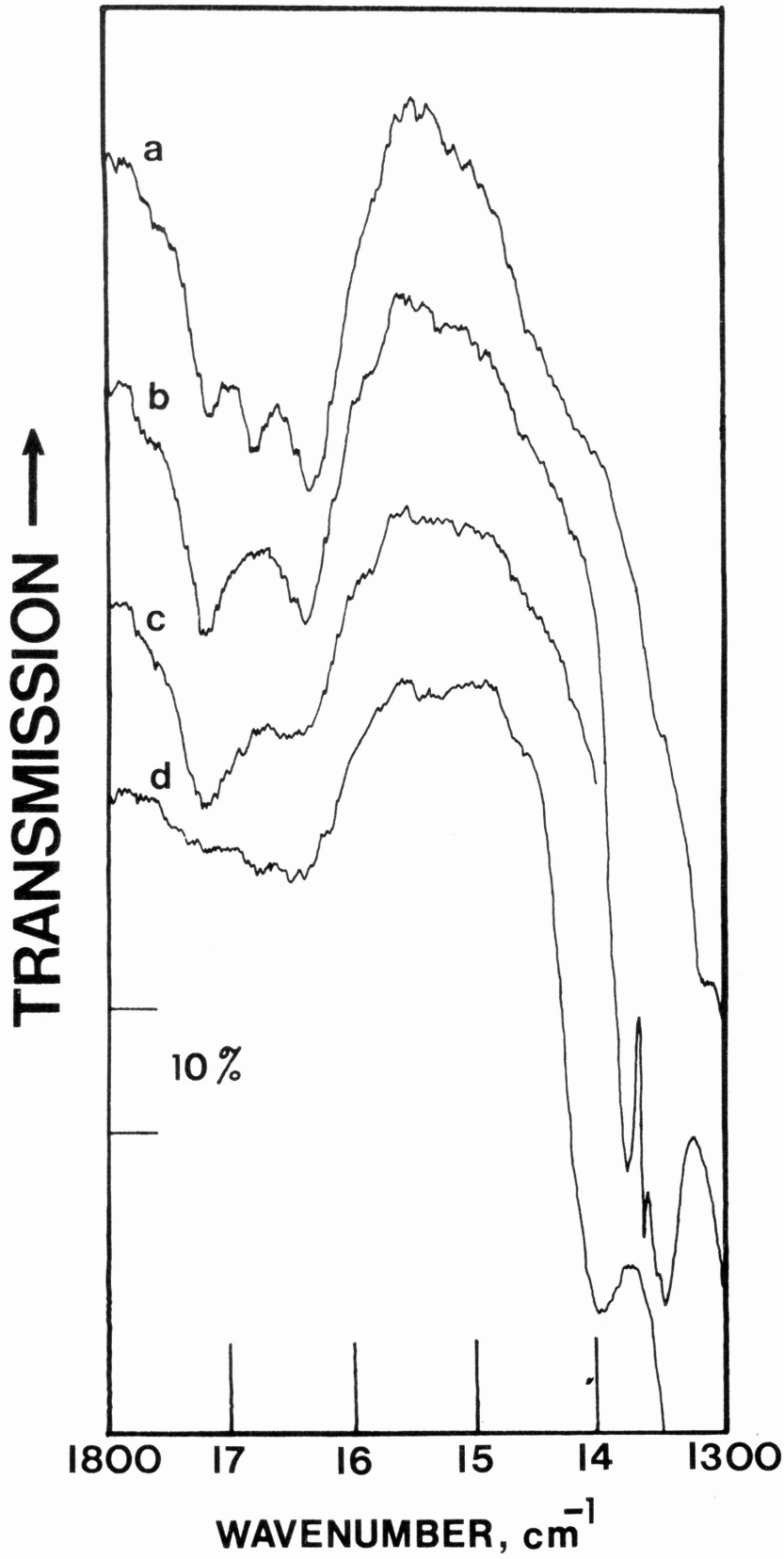
a
b
c
d
TRANSMISSION
10 %
1800
17
16
15
14
1300
WAVENUMBER, cm^{-1}

1396 cm^{-1}. Photoelectron spectra collected after the infrared experiment were of low intensity but were similar to Figure 4a.

Results using higher reactant pressures are further exemplified in Figure 8, which shows a sequence of spectra similar to Figure 6 for a hydrated silica alumina sample. The silica alumina background spectrum, curve a, shows a strong band at 1450 cm^{-1} which is attributed to NH_4^+ ions formed from ammonia adsorption from the laboratory atmosphere during sample preparation. The band was removed only by degassing at 375° or higher temperatures for several hr. The band at 1336 cm^{-1}, curve b, was stable on the more acidic surface without the presence of an appreciable amount of gas phase SO_2, but the band could be removed by brief evacuation at 25°. The peak was largely removed after admitting NO_2-N_2O_4, curve c, and other bands appeared at 1315(sh), 2275, and 1650-1730 cm^{-1}. Curiously the 1450 cm^{-1} peak decreased in intensity, shifted to lower frequency, and finally vanished during the reaction and subsequent evacuation. The peak was only partially removed with lower NO_2 pressures. Degassing at 25° for 4 hr, curve e, produced a band at 1398 cm^{-1} and shifted the adsorbed water peak by 18 cm^{-1} to a higher frequency. The bands at 2285 and 1398 cm^{-1} disappeared after adsorbing water vapor; and, only the 1398 cm^{-1} peak was restored by further outgassing at 25°.

As illustrated in Figure 9, somewhat different behavior was observed when the gases were adsorbed on $SiO_2 \cdot Al_2O_3$ in reverse order. Distinct bands appeared at 1320 and 1672 cm^{-1}, curve b, after initial exposure to NO_2-N_2O_4. These bands were slowly removed by evacuation at 25°, and nothing appeared in the 1500-1600 cm^{-1} region. However,

Figure 8. Infrared spectra of SO_2 and NO_2 on hydrated $SiO_2 \cdot Al_2O_3$: (a) background; (b) 7 Torr SO_2 admitted one hour with excess removed by expansion; (c) 15 Torr NO_2 admitted; (d) 4 hr later; (e) degassed at 25°, 4 hr.

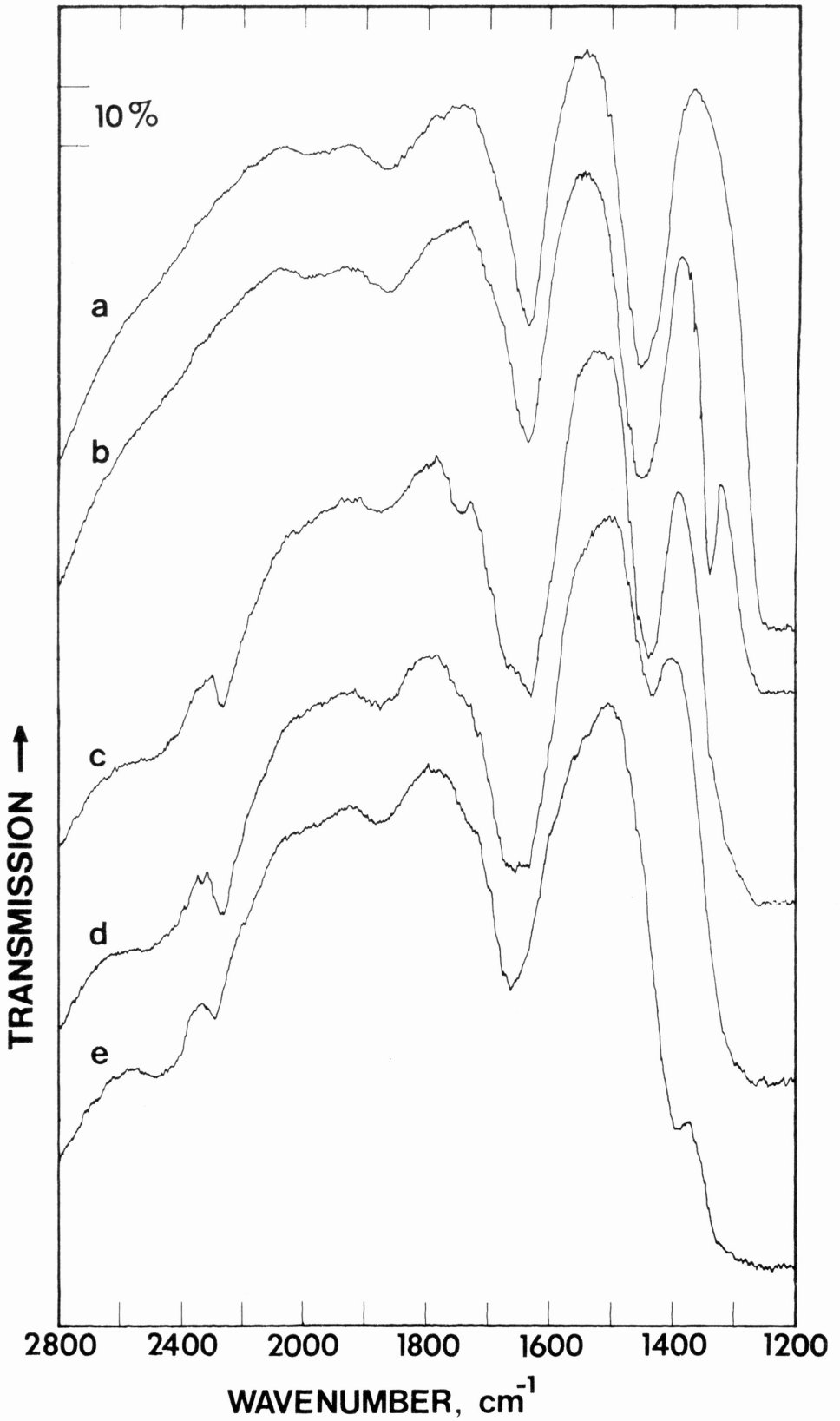
10%
a
b
c
d
e
TRANSMISSION
2800
2400
2000
1800
1600
1400
1200
WAVENUMBER, cm-1

after the sample was allowed to stand in NO_2-N_2O_4 for several hr and subsequently degassed for 3 hr at 25°, curve d, new bands were observed at 1590 and 1545(broad) cm^{-1} in addition to residual shoulders at 1318, 1665, and 1730 cm^{-1}. Upon admitting 7 Torr SO_2, curves e, f, and g, these bands all slowly vanished, whereas low intensity peaks appeared at 1336 and 2280 cm^{-1}. The band due to the bending mode of adsorbed water was also broadened, shifted to higher frequency, and not affected further by degassing at 25°. The band at 2280 cm^{-1} was never resolved when hydrated silica with adsorbed NO_2 was reacted with SO_2.

In an effort to detect adsorbate bands below 1200 cm^{-1} powdered oxide samples were reacted with SO_2 and NO_2 in the usual manner and subsequently diluted into KCl pellets. As depicted in Figure 10, this procedure provided enhanced transmission in the region below 1050 cm^{-1} and consequently allowed several additional bands to be distinguished. The frequencies and assignments of the observed bands are summarized in Table II. Unfortunately, the 1050-1270 cm^{-1} region remained obscured.

Comparative infrared experiments were carried out with samples dehydrated <u>in vacuo</u> to 500° in order to explore the significance of adsorbed water. No interaction of SO_2, NO_2, or SO_2 and NO_2 with dehydrated SiO_2 could be detected. Further addition of a trace of water vapor, however, produced a band at 2280 cm^{-1}, and continued exposure to water vapor dissipated this peak and produced bands at 1315(sh), 1635, and 1680 cm^{-1}. In contrast, on dehydrated $SiO_2 \cdot Al_2O_3$, SO_2 physisorbed to a small extent as indicated by the band at 1336 cm^{-1}; and, as shown in Figure 11, NO_2 was strongly adsorbed. The intensity of the 1590 and 1650 cm^{-1} bands decreased in a manner proportional to time

Figure 9. Infrared spectra of NO_2 and SO_2 on $SiO_2 \cdot Al_2O_3$: (a) background; (b) 16 Torr NO_2-N_2O_4 admitted; (c) 24 hr later; (d) degassed at 25° 3 hr; (e), (f), and (g) immediately, 1 hr, and 2.5 hr after admitting 8 Torr SO_2; (h) degassed overnight at 25°.

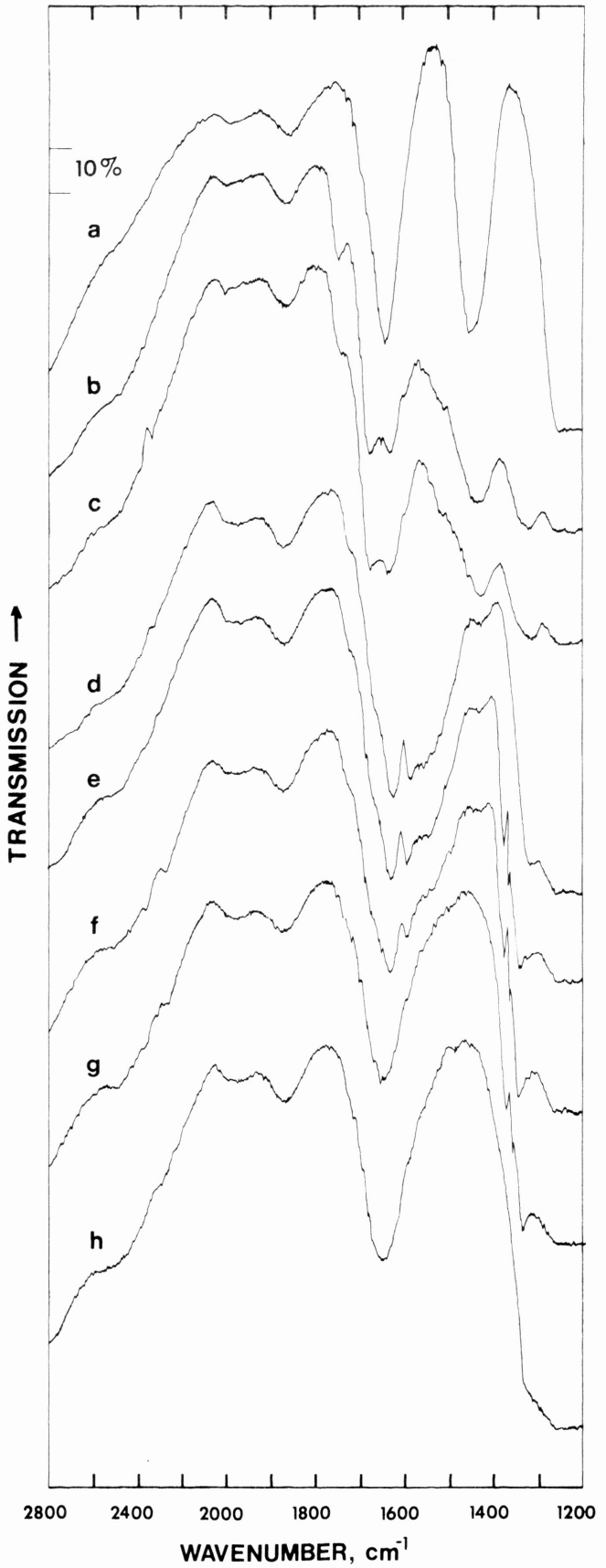
10%
a
b
c
d
e
f
g
h
TRANSMISSION
2800
2400
2000
1800
1600
1400
1200
WAVENUMBER, cm-1

Figure 10. Low frequency region infrared spectra of SiO_2 and $SiO_2 \cdot Al_2O_3$ diluted in KCl after reaction with SO_2 and NO_2: (a) SiO_2 background; (b) -SiO_2,---$SiO_2 \cdot Al_2O_3$.

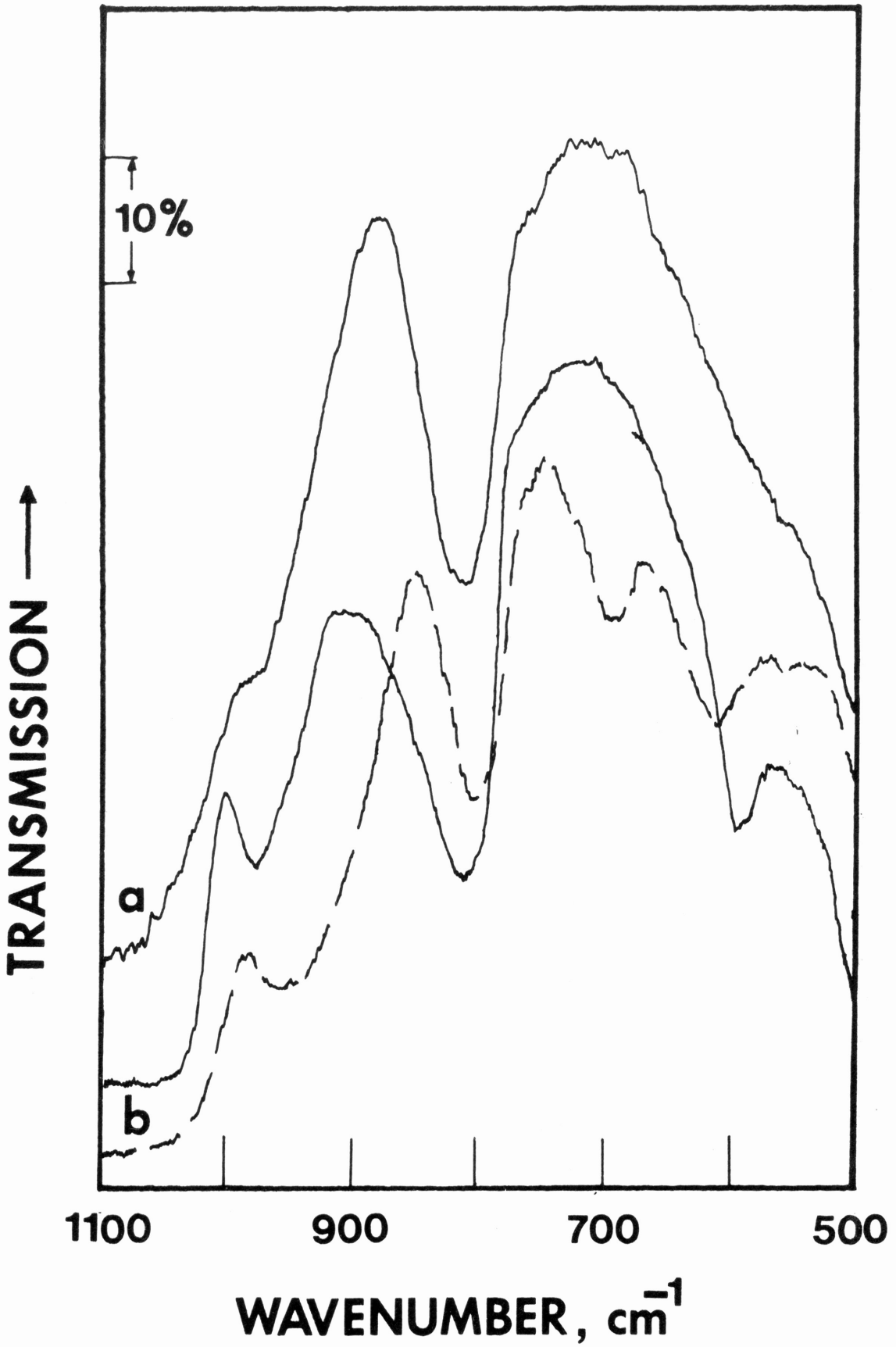
10%
TRANSMISSION
a
b
1100
900
700
500
WAVENUMBER, cm^{-1}

Table II. Observed Frequencies of Adsorbed Species (cm^{-1})[a]

Adsorbate	SiO_2	$SiO_2 \cdot Al_2O_3$	Description
H_2O	1635	1635	υ_2 phys. ads. H_2O
SO_2	1337	1336	υ_3 phys. ads. SO_2
N_2O_4	1735	1730	υ_9-υ(NO) phys. ads. N_2O_4
NO_2	1315(sh)	1320	$\upsilon_2(A_1)$ 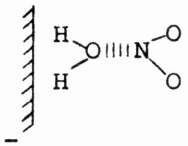 phys. ads.
	1680	1672	$\upsilon_4(B_2)$
	-	690	$\upsilon_3(A_1)$
	1420	1420(sh)	υ_3 NO_3^-
	-	1545	$\upsilon(A_1)$ bidentate Nitrato Species
	-	1590	υ_{NO_2} antisym. $\geqslant$Si-O-N 
	-	1650[(b)]	$\upsilon_{N=O}$ $\geqslant$Si-O
$SO_2 + NO_2$	595	610	υ_4 $SO_4^=$
	975	960	υ_1 $SO_4^=$
	2460	2465	υ_{O-H} sym. H_2SO_4
	2280	2270	υ_1 NO^+
	1400	1398	υ_1 NO_2^+

sh = shoulder

(a) ± 5 cm^{-1}

(b) only on $SiO_2 \cdot Al_2O_3$ degassed to 500°

Figure 11. Infrared spectra of NO_2 and SO_2 on degassed $SiO_2 \cdot Al_2O_3$: (a) background; (b) 3 Torr No_2 admitted; (c) degassed 15 min at 25°; (d) and (e) immediately and 1.5 hr after admitting 1.5 Torr SO_2; (f) 3 Torr D_2O admitted.

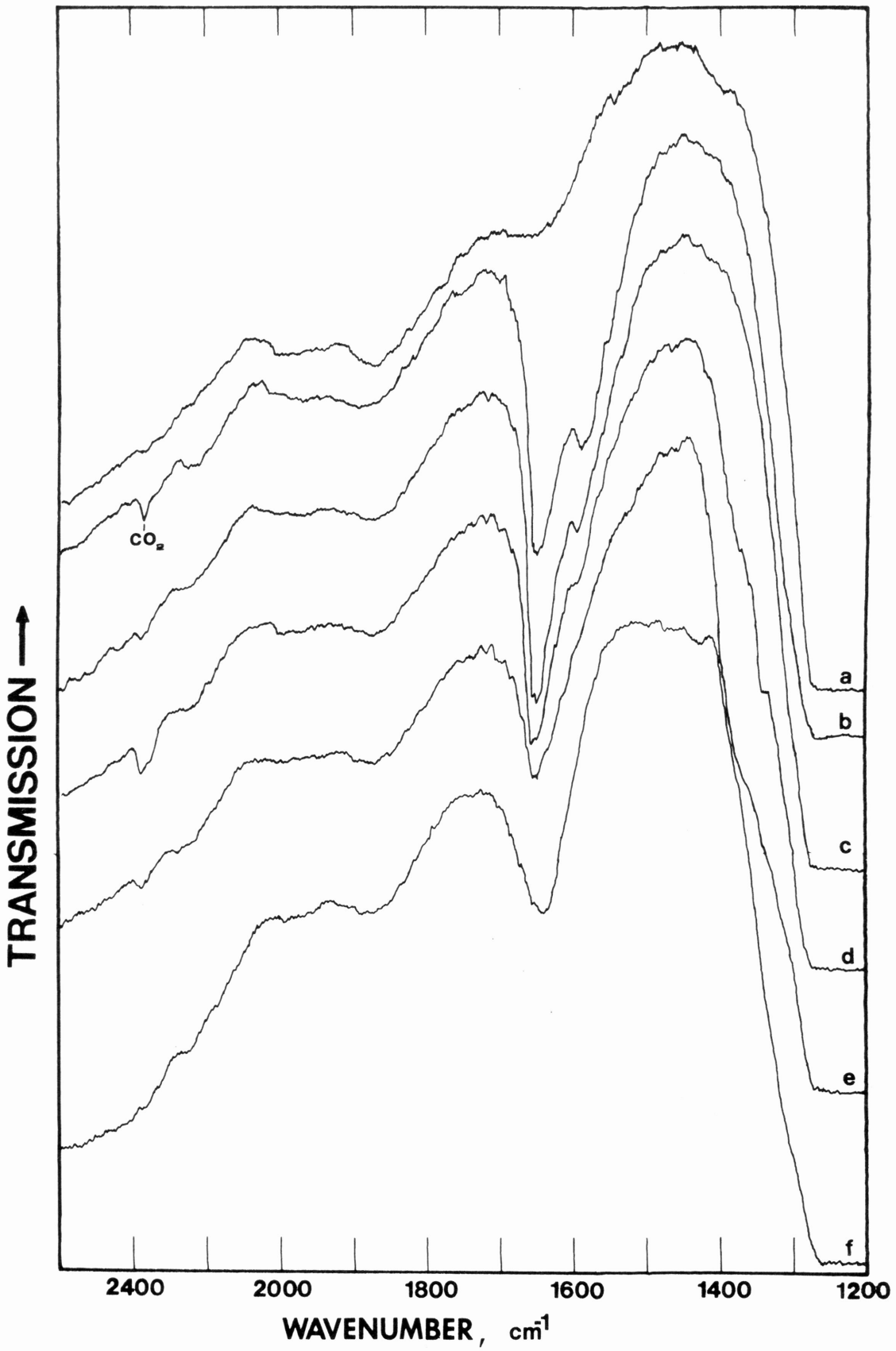
TRANSMISSION
WAVENUMBER, cm-1
2400
2000
1800
1600
1400
1200
CO2
a
b
c
d
e
f

when a low pressure of SO_2 was admitted, and addition of D_2O produced no additional changes. Photoelectron spectra revealed very low intensity lines at 169.3, 400.5-403, and 407.5 eV.

Similar EPR experiments were attempted under a number of conditions to determine if one or more of the reacting species were radicals. The spectrum of the adsorbed NO_2 molecule was the only observable signal, and a typical spectrum for NO_2 adsorbed on hydrated $SiO_2 \cdot Al_2O_3$ is shown in Figure 12. The g values and hyperfine splitting constants for NO_2 on hydrated silica and silica alumina are summarized in Table III and are very similar to those reported for NO_2 adsorbed on MgO (28). As expected, the NO_2 signal vanishes about 1 hr after exposure to 5 Torr SO_2 at 25°.

Figure 12. EPR of NO_2 adsorbed on hydrated $SiO_2 \cdot Al_2O_3$: 10 Torr admitted 30 minutes, excess evacuated.

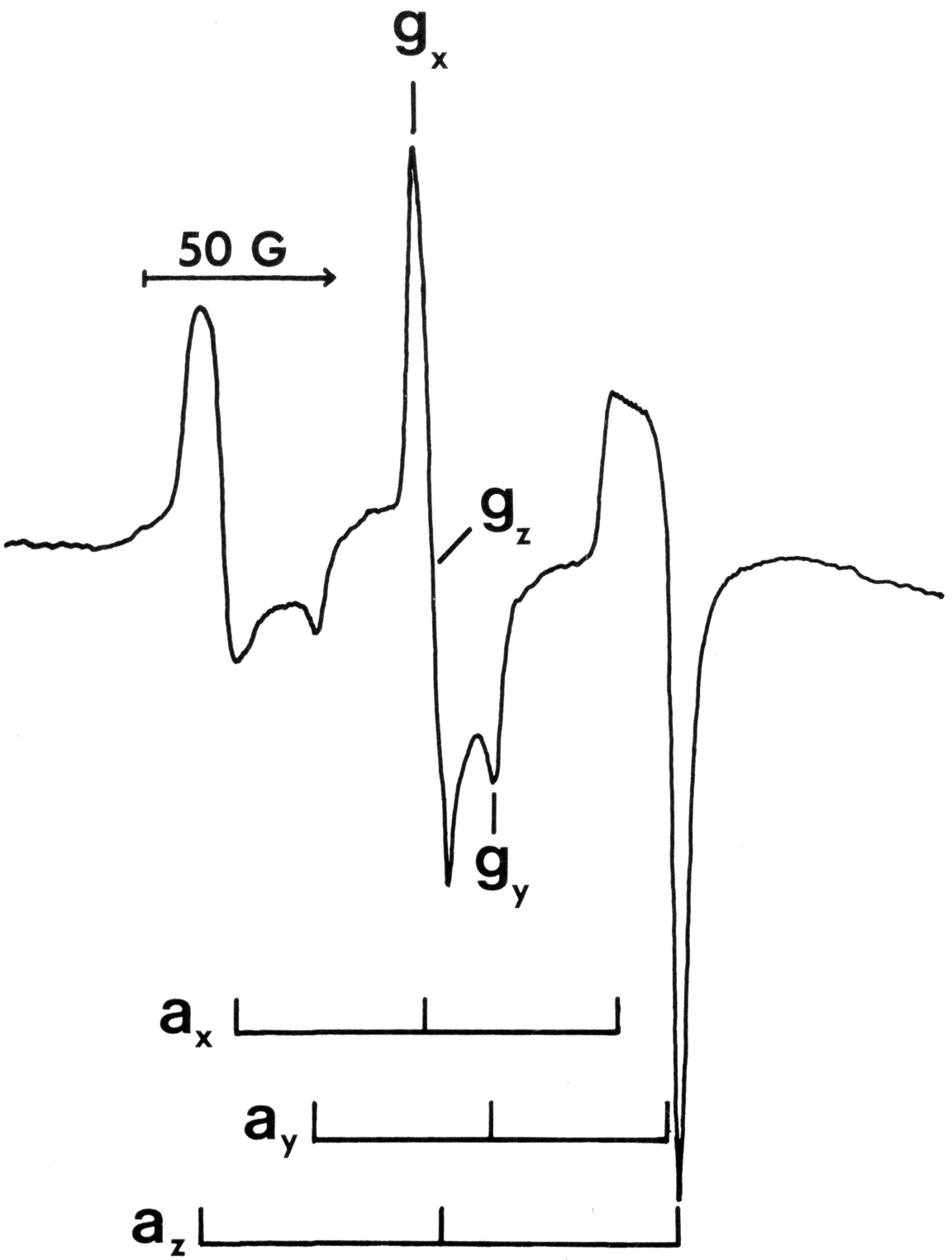
g_x
50 G
g_z
g_y
a_x
a_y
a_z

Table III. EPR Parameters[a] for Adsorbed NO_2

Adsorbent	g_x	g_y	g_z	A_{iso}[b] (G)	A_x	A_y	A_z
$SiO_2 \cdot xH_2O$	2.005	1.994	2.003	53.2	-3.7	-6.2	9.8
$SiO_2 \cdot Al_2O_3 \cdot xH_2O$	2.006	1.993	2.003	54.5	-3.5	-6.5	10.0
MgO[c]	2.005	1.992	2.002	56.5	-3.5	-7.5	10.9

(a) g values ±0.001, A values ±0.5 G

(b) $A_{iso} = 1/3(a_x + a_y + a_z)$

(c) Ref. 28

DISCUSSION

In order to place in context the specific observations which form the main subject of this discussion, a few prefatory, general remarks are appropriate. First, NO_2 exists in a highly temperature and pressure dependent equilibrium with its dimer, N_2O_4. At pressures below 3-4 Torr N_2O_4 is largely dissociated; however, at pressures above about 10 Torr and at 25°C both species exist in significant concentrations.

Second, an extensive volume of literature is available regarding infrared absorption and x-ray photoemission by adsorbed oxides of sulfur and nitrogen. The vibrational frequencies, and to a lesser extent the binding energies, of these species are very sensitive to the bonding of the adsorbate with the surface. Although meaningful assignments may be facilitated by comparing frequencies and binding energies of known compounds, emphasis must also be placed, as has been the approach here, on the dynamic equilibria that exist between adsorbed species and molecules in the gas phase.

Identification of Adsorbed Species

The slow appearance of the 1735 cm^{-1} infrared band paralleled that of the 400.5 eV N(1s) photoelectron line. Both features were favored by higher NO_2-N_2O_4 pressures, and the species responsible for these features was slowly desorbed at 25°. Since the infrared band at 1735 cm^{-1} formed as the 1748 cm^{-1} gas phase N_2O_4 band disappeared, the former is attributed to rather strongly physically adsorbed N_2O_4. This species had a surprisingly low reactivity towards SO_2 (Figure 7) indi-

cating that N_2O_4 is immobilized at the surface via strong hydrogen bonding with adsorbed water and surface -OH groups.

The bands observed near 1315 and 1680 cm^{-1} after adsorption of NO_2 (Figures 6,7 and 9) are assigned to a reversibly formed nitric acid-like surface species. The antisymmetric and symmetric stretching frequencies of the NO_2 group of nitric acid occur at 1680 and 1308 cm^{-1} (29), and these are the most intense of several infrared absorptions. The surface species was rapidly desorbed at 25° from silica and more slowly desorbed from $SiO_2 \cdot Al_2O_3$. Association is apparently stronger on the more acidic silica alumina. The species was very reactive with SO_2 on both surfaces. The broad shoulder observed near 1420 cm^{-1}, which sharpened with outgassing at 100°, confirms that NO_2 may interact further to actually form nitric acid which is ionizable on the hydrated surfaces. This band is attributed to adsorbed nitrate ions, and this interpretation is entirely consistent with the observed N(1s) photoelectron line with a 407.3 eV binding energy. The nitrate ion in NH_4NO_3 and surface nitrates formed by adsorbing NO_2 on NiO (30) have binding energies of 407.2 eV.

The 2280 cm^{-1} absorption could be produced in two ways; by adsorbing NO_2 on dehydrated silica alumina or by reacting SO_2 and NO_2 on the hydrated surfaces. This peak is assigned to ionically bound NO^+; and, as will be subsequently shown, this species is an important intermediate in the surface oxidation of SO_2. In $NOBFCl_3$ the cationic NO absorbs at 2335 cm^{-1} (31). The tremendous shift of the N-O stretching frequency by 400 cm^{-1} in going from gas phase NO (1876 cm^{-1}) to NO^+ is well known and arises from loss of an electron from a π antibonding

molecular orbital. In this work NO^+ was present in low concentrations, and it was vulnerable to surface hydrolysis. Accordingly, no unambiguous N(1s) binding energy may be advanced. However, Finn and Jolly (32) and Mingos and Ibers (33) have reported N(1s) binding energies of 400-402 eV for a large number of coordinated nitrosyls, some of which are essentially cationic. If NO^+ is present in our ESCA spectra, it is obscured by photoemission from other groups with similar binding energies. Dianis has suggested that NO^+ with no π-back bonding with the adsorbent should have a binding energy near 401 eV (34).

Bands were also observed at 1650 and 1590 cm^{-1} when NO_2 was adsorbed on $SiO_2 \cdot Al_2O_3$ dehydrated to 500° (Figure 11). Chao and Lunsford (35) attributed similar bands observed after adsorption of NO_2 on a decationated Y-type zeolite to nitrite groups covalently bound to trigonal Si^+ centers. In the present work the peak at 1590 cm^{-1} as well as an additional broad band at 1545 cm^{-1} were also formed when hydrated $SiO_2 \cdot Al_2O_3$ with adsorbed NO_2 was degassed at 25° several hours (Figure 9). The absence of the 1650 cm^{-1} band suggests that the 1590 and 1650 cm^{-1} peaks are due to two different species. Organic nitrites and nitrates absorb strongly in the 1650-1680 and 1610-1650 cm^{-1} regions, respectively (36). It seems rather likely that the 1590 and 1650 cm^{-1} bands correspond with the antisymmetric $-NO_2$ and -N=O stretching frequencies of nitrates and nitrites, respectively, covalently bound to silicon atoms of the lattice. The band at 1545 cm^{-1} is consistent with a bidentate nitrato species (37). Further detailed justification for these assignments has been given by Blyholder and Allen (38). It is noteworthy that these strongly bound oxides of

nitrogen all exhibited a substantial reactivity with SO_2.

The infrared and ESCA data provide compelling evidence for the formation of sulfuric acid on both surfaces. The close agreement of the S(2p) and S(2s) ESCA spectra on SiO_2 and $SiO_2 \cdot Al_2O_3$ with that of $(NH_4)_2SO_4$ and other sulfates (39) is rather convincing evidence for the occurence of adsorbed sulfur in only one chemical state; i.e. the +6 oxidation state. Sulfite ions and lower sulfur oxidation states have S(2p) binding energies of 168 eV or less. The broad infrared band observed near 2460 cm^{-1} is in good agreement with the O-H symmetric stretching frequency of sulfuric acid at 2450 cm^{-1} (40). The fact that this band was resolved only after the sample was degassed following the reaction indicates that sulfuric acid is largely ionized on the hydrated surfaces. This interpretation is consistent with the spectra observed in the 500-1100 cm^{-1} region. The free sulfate ion has T_d point symmetry; and, consequently, its υ_3 and υ_4 vibrations are infrared active near 1105 and 611 cm^{-1} (31). When the ion is coordinated through one oxygen the forbidden υ_1 vibration is allowed near 970 cm^{-1}, and the triply degenerate υ_3 mode splits into two bands. The symmetry is lowered further to C_{2v} in bidentate sulfates, and, thus, three bands are expected from splitting of the υ_3 vibration in addition to the one υ_1 frequency. Low transmission precluded detection of the υ_3 frequencies, but the bands observed near 600 and 970 cm^{-1} suggest that sulfate anions are present on the surfaces. Additional absorption in the 1040-1050 cm^{-1} region may be ascribed to bisulfate anions.

The 1400 cm^{-1} infrared band and 401.2 eV N(1s) photoelectron line are assigned to adsorbed NO_2^+. Interaction with the surface lowers the

$D_{\infty h}$ symmetry of the cation and allows the normally Raman-active symmetric stretching vibration to become infrared active. The antisymmetric stretching and degenerate bending frequencies occur near 2360 and 570 cm^{-1}, respectively (31). The former was presumably not observed because it was masked by the absorption due to atmospheric CO_2 which was balanced out of the spectrum. Nitrate ions also absorb around 1400 cm^{-1}; however, nitrate ions have N(1s) binding energies $\gtrsim$ 407 eV. Failure to observe a line in this region, coupled with the appearance of a single line due to a strongly adsorbed species at 401.2 eV following the surface reaction, suggests that nitronium ions are stabilized on the surfaces with adsorbed H_2SO_4. Further evidence for this formulation was derived from infrared studies in which NO_2BF_4 vapor was adsorbed onto hydrated SiO_2 before and dehydrated SiO_2 after reaction with SO_2 and NO_2. In the former case adsorbed nitric acid (1680 and 1310 cm^{-1}) was formed. In the latter, however, the 1400 cm^{-1} band was intensified and a shoulder of very low intensity appeared near 2370 cm^{-1}. ESCA spectra of these samples showed single N(1s) lines at 407.3 and 401.2 eV, respectively. There is little question that these features are due to adsorbed NO_2^+.

Formation of Adsorbed Species

Dehydration, deamination, and dehydroxylation of $SiO_2 \cdot Al_2O_3$ at 500° to form trigonal Si^+ centers may be represented to proceed according to

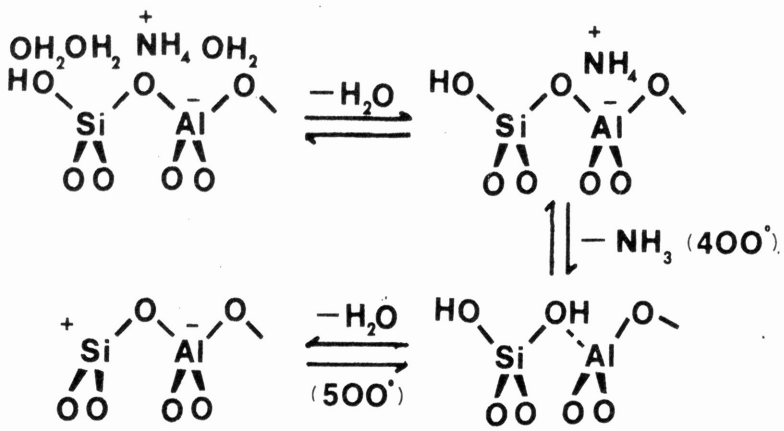

The diamagnetic nature of the surface species assigned above and the unusual, $^2A_1$, electronic ground state of the NO_2 molecule require that some subtle charge transfer equilibria occur upon adsorption of NO_2. In particular, formation of nitrites on Si^+ sites requires that an electron be gained from the lattice or another NO_2 molecule. The latter seems likely since NO_2 may adsorb on $\geqslant Si\text{-}O^-$ sites with loss of an electron to form covalent nitrates. At present, it is not clear how NO^+ is stabilized on dehydrated $SiO_2 \cdot Al_2O_3$.

Of paramount interest in the present work, however, is the mechanism by which SO_2 is oxidized to sulfuric acid on the hydrated surfaces. Dynamic equilibria among adsorbed species are summarized in the scheme below:

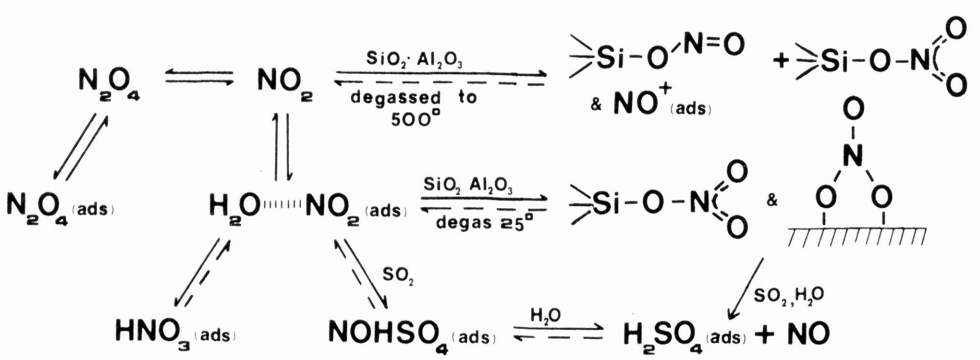

The nitric acid-like species described earlier was the most reactive of several adsorbed oxides of nitrogen. Reaction with SO_2 is believed to produce $NOHSO_4$. Oxidation probably involves nucleophillic attack by NO_2 upon the coordinatively unsaturated SO_2 molecule. Water, by very rapid or concerted addition to adsorbed SO_2, effects stabilization of the transition state leading to oxide transfer. The importance of water is borne out by the fact that no reaction was detected on dehydrated SiO_2, and different reactions occurred on dehydrated $SiO_2 \cdot Al_2O_3$. Nitrosonium bisulfate is further hydrolyzed on the surfaces to form adsorbed sulfuric acid and gas phase NO. Mass spectral analysis of residual gases, evolved following a typical experiment, confirmed that NO was produced in the reaction. Although direct proof for $NOHSO_4$ as an intermediate is lacking, the experimental evidence strongly favors this interpretation.

Nitrosonium bisulfate is an important intermediate in the gas phase oxidation of SO_2 to H_2SO_4 with NO_2 and water at high pressures and temperatures; e.g. the lead chamber process incorporates this reaction (41). The observation that the NO^+ infrared band was distinctly detected only with relatively high NO_2 pressures (~ 10 Torr), suggests that NO^+ is usually present in low steady state concentrations. Furthermore, shifts of the adsorbed water bending band to higher frequencies during dehydration following the reaction indicate an increase in hydrogen bonding and, undoubtedly, a strongly acidic surface environment.

The nature of the interaction between the more strongly bound nitrates and nitrites with SO_2 on $SiO_2 \cdot Al_2O_3$ is less obvious. Ammonia is evidently displaced from the surface by NO_2 which is adsorbed

strongly, whereas SO_2 has no effect on the 1450 cm^{-1} band. The reaction between strongly bound nitrates and SO_2 on partially dehydrated $SiO_2 \cdot Al_2O_3$ (Figure 9) appeared to involve NO^+, and it seems likely that this reaction is similar to that described above for SiO_2.

Nitronium ions are stabilized on the acidic surfaces by degassing the sample following the surface reaction. Nitronium and nitrosonium ions are strong oxidants and, thus, readily hydrolyzed in solution (42).

$$NO_2^+ + 2H_2O \rightleftharpoons NO_3^- + H_3O^+ \quad (3)$$

$$NO^+ + 2H_2O \rightleftharpoons HNO_2 + H_3O^+ \quad (4)$$

The HNO_2 decomposes further (43)

$$3HNO_2 \rightleftharpoons NO_3^- + H_3O^+ + 2NO \quad (5)$$

Similar mechanisms are apparently operative on hydrated silica and silica alumina with adsorbed H_2SO_4. Dehydration shifts the acid base equilibria so that NO_2^+ may be formed reversibly from adsorbed nitrate ions or nitric acid

$$2H_2SO_4 \cdot xH_2O + HNO_3 \cdot yH_2O \underset{+H_2O}{\overset{-H_2O}{\rightleftharpoons}} NO_2^+ + H_3O^+ + 2HSO_4^- \quad (6)$$

Surface hydrolysis of NO^+, however, is facile on SiO_2, slower on $SiO_2 \cdot Al_2O_3$, and irreversible on both surfaces. Ionization of dinitrogen tetroxide in concentrated sulfuric acid is also well known (42).

$$N_2O_4 + 3H_2SO_4 \rightleftharpoons NO^+ + NO_2^+ + 3HSO_4^- + H_3O^+ \quad (7)$$

It seems likely that adsorbed N_2O_4 may similarly ionize in the acidic surface monolayer during dehydration. Although suggestive, irreversible ionization of adsorbed N_2O_4 would in part account for the significant intensity of the infrared band at 1400 cm^{-1}.

The striking attenuation of the Si(2s and 2p) lines compared with

with corresponding Al(2s and 2p) lines on a number of $SiO_2 \cdot Al_2O_3$ samples following the reaction probably arises from one of two possible effects. The surface geometry may be modified during reaction so that AlO_{3-4} groups are drawn to the surface with diffusion of SiO_4 groups into the bulk amorphous oxide. Alternatively, sulfate anions may preferentially migrate to and concentrate on silicate regions of the surface. Both effects could occur simultaneously. The latter, however, would require a high ionic mobility and, considering the similar Si- and Al(2s) photelectron escape depths (~ 20Å), packing of sulfate ions on top of one another. Appreciable mobility is expected on the hydrated surfaces, but ionic or molecular packing seems unlikely. The possibility that surface hydrates or clathrates are formed was ruled out by the absence of photoemission from the la_1 molecular level (mainly O(2s)) of strongly adsorbed water at ca. 32 eV.

CONCLUSIONS

The heterogeneous oxidation of SO_2 to adsorbed sulfuric acid with NO_2 and adsorbed oxides of nitrogen occurs at 25° on hydrated silica and silica alumina. Nitrosonium ions are an intermediate in this oxidation reaction, and nitronium cations may be stabilized on the acidic surfaces following the reaction. Similar reactions are expected to occur among air pollutants on the surfaces of particulates suspended in the atmosphere.

REFERENCES

1. P. G. Maurin and J. Jonakin, Chem. Engr., Desk Issue, 173 (1970).

2. C. M. Shy and J. F. Finklea, Environ. Sci. Technol., 7, 204 (1973).

3. R. Prince and F. F. Rose, Water, Air, and Soil Pollution, 1, 286 (1972).

4. T. Novakov, P. K. Mueller, A. E. Alcocer, and J. W. Otvos, J. Colloid Interface Sci., 39, 225 (1972).

5. N. L. Craig, A. B. Harker, and T. Novakov, Atmos. Environ., 8, 15 (1974).

6. L. D. Hulett, T. A. Carlson, B. R. Fish, and J. L. Durham, "Determination of Air Quality", G. Mamantov and W. D. Shults, Eds., Plenum Press, N.Y., 1972, p. 179.

7. J. H. Lunsford, to be published.

8. M. J. D. Low, A. J. Goodsel, and N. Takezawa, Environ Sci. Technol., 5, 1191 (1971).

9. R. A. Schoonheydt and J. H. Lunsford, J. Catal., 26, 261 (1972).

10. M. J. Lin and J. H. Lunsford, J. Phys. Chem., 79, 892 (1975).

11. M. J. Lin, Ph.D. Dissertation, Texas A&M University, May 1976.

12. A. V. Deo, I G. Dalla Lana, and H. W. Habgood, J. Catal., 21, 270 (1971).

13. J. Pearce and J. H. Lunsford, unpublished results.

14. R. A. Schoonheydt and J. H. Lunsford, J. Phys. Chem., 76, 323 (1972).

15. Y. Ono, H. Tokunaga, and T. Keii, J. Phys. Chem., 79, 752 (1975).

16. K. V. S. Rao and J. H. Lunsford, J. Phys. Chem., 78, 649 (1974).

17. A. K. Kolosov, V. A. Shvets, and V. B. Kazanskii, J. Catal., 37, 387 (1975).

18. N. A. Renzetti and G. J. Doyle, Int. J. Air Pollut., 2, 327 (1960).

19. S. Jaffee and F. S. Klein, Trans. Faraday Soc., 62, 2650 (1966).

20. Y. Bourbigot, J. Bricard, G. Madelaine, and D. Vigla, Comp. Rend. Acad. Sci. Paris, 276, 547 (1973).

21. C. Canosa, W. G. Philby, and R. D. Penzhorn, J. Environ Sci. Health, 1, 93 (1976).

22. L. H. Little, "Infrared Spectra of Adsorbed Species", Academic Press, N. Y., 1966.

23. M. L. Hair, "Infrared Spectroscopy in Surface Chemistry", Marcel Dekker Inc. N. Y., 1967.

24. W. N. Delgass, T. R. Hughes, and C. S. Fadley, Catal. Rev., 4, 179 (1970).

25. J. S. Fritz and G. H. Shenk, "Quantitative Analytical Chemistry", 2nd Ed., Allyn and Bacon, Inc., Boston, 1969, p. 509.

26. K. Siegbahn, D. Hammond, H. Fellner-Feldegg, and E. F. Barnett, Sci., 176, 245 (1972).

27. Written by L. E. Cox, University of Georgia; modified by M. J. Lin, Texas A&M University.

28. J. H. Lunsford, J. Colloid Interface Sci., 26, 355 (1968).

29. R. A. Marcus and J. M. Fresco, J. Chem. Phys., 27, 564 (1957).

30. W. E. Swartz and M. Youssefi, J. Elec. Spec., 8, 61 (1976).

31. K. Nakamoto, "Infrared Spectra of Inorganic and Coordination Compounds", Wiley, N. Y., 1963.

32. P. Finn and W. L. Jolly, Inorg. Chem., 11, 1050 (1972).

33. D. M. P. Mingos and J. A. Ibers, Inorg. Chem., 9, 1105 (1970).

34. W. P. Dianis, Ph.D. Dissertation, Northwestern University, May 1974.

35. C. C. Chao and J. H. Lunsford, J. Amer. Chem. Soc., 93, 71 (1971).

36. J. B. Lambert, H. F. Shurvell, L. Verbit, R. G. Cooks, and G. H. Stout, "Organic Structural Analysis", Macmillan, Inc., N. Y., 1976.

37. C. C. Addison and B. M. Gatehouse, J. Chem. Soc., 613 (1960).

38. G. Blyholder and M. C. Allen, J. Phys. Chem., 70, 352 (1966).

39. B. J. Lindberg, K. Hamrin, G. Johansson, N. Gelius, A. Fahlman, C. Nording, and K. Siegbahn, Phys. Scripta, 1, 286 (1970).

40. R. J. Gillespie and E. A. Robinson, Can. J. Chem., 40, 644 (1962).

41. R. C. Brasted, "Comprehensive Inorganic Chemistry", Vol. 8,

D. Van Nostrand, Inc., Princeton, N. J., 1961.

42. C. K. Ingold and D. Miller, J. Chem. Soc., 2612 (1950), and references cited therein.

43. F. A. Cotton and G. Wilkinson, "Advanced Inorganic Chemistry", 3rd Ed., Wiley, N. Y., 1972.